# Yield Estimation of Major Crops in Butuan City, Agusan del Norte Using Geospatial Techniques

Edgardo Ricardo B. Sajonia Jr
Department of Electronics Engineering, Caraga State University (CSU DECE)

Anamarie P. Sajonia
College of Engineering and Geosciences, Caraga State University (CSU CEGS)

https://doi.org/10.5109/7323281

出版情報：Proceedings of International Exchange and Innovation Conference on Engineering & Sciences (IEICES). 10, pp.325-331, 2024-10-17. International Exchange and Innovation Conference on Engineering & Sciences
バージョン：

# Yield Estimation of Major Crops in Butuan City, Agusan del Norte Using Geospatial Techniques

Edgardo Ricardo B. Sajonia Jr.[1 2 3], Anamarie P. Sajonia[3 4 5]
[1]Department of Electronics Engineering, Caraga State University (CSU DECE)
[2]Center for Renewable Energy, Automation, and Fabrication Technology (CSU CRAFT)
[3]College of Engineering and Geosciences, Caraga State University (CSU CEGS)
[4]Department of Agricultural and Biosystems Engineering, Caraga State University (CSU DABE)
[5]Center for Resource Assessment Analytics and Emerging Technologies (CSU CREATE)
Corresponding author email: ebsajonia@carsu.edu.ph

**Abstract:** *This study uses LiDAR derivatives and Landsat 8 OLI/TIRS for yield estimation of major crops in Butuan City, Agusan del Norte, Philippines. Yield estimation is crucial for crop management, food security, and economic impact. Remote sensing techniques and GIS were used for crop yield estimation. eCognition software classified photos, while LiDAR derivatives like Canopy Height Model (CHM), Digital Surface Model (DSM), and Normalized Digital Surface Model (nDSM) were produced. Vegetation objects were classified into High, Medium, and Low Elevation Groups based on LiDAR nDSM heights. Regression analysis developed the allometric equation for yield estimation. The study achieved 94.36% overall accuracy in map classification and yield estimations of 84.5% for banana, 87.9% for coconut, 72.5% for corn, and 86.4% for mango. Average production was 58.414 tons/ha for bananas, 1,001.15 tons/ha for coconut, 8.48 tons/ha for corn, and 1.256 tons/ha for mango.*

**Keywords:** Food security; LiDAR derivatives; Landsat 8 OLI/TIRS; Yield estimation; Allometric equation.

## 1. INTRODUCTION

Agriculture remains a significant contributor to the GDP, overall employment, and the means of subsistence for the rural population. It is also the nation's main source of income, with impoverished households experiencing the worst levels of food insecurity. The country's agricultural development has great potential in Mindanao. Providing more over 40% of the nation's food needs and making up over 30% of the national food commerce, it is regarded as the food basket of the nation[1]. However, the negative effects of climate change on agriculture and the growing population's demand for food make ensuring food security in the nation a significant concern.

According to [2], changes in climatic elements will affect agricultural production. The rising temperatures eventually lead to lower yields of desired crops while promoting the growth of weeds and pests. Furthermore, variations in precipitation patterns raise the risk of both long-term production decreases and short-term crop failures. Global food security is at risk due to the general negative effects of climate change on agriculture, even though particular crops may prosper in some parts of the world [3]. It was predicted that yields for crops of East Asia and the Pacific in 2050 will decline by 4% for maize because of climate change [4]. Furthermore, the report of [5], under mild El Niño circumstances, the country's total agricultural production losses might be P8.09 billion, while during a severe dry spell, they could reach P20.46 billion.

Hence, estimating crop yields is crucial both at national and regional levels. Planners and decision-makers can forecast how much to import in the event of a shortage or export in the event of a surplus thanks to crop yield estimation. Furthermore, it permits the government to do tactical backup plans for redistributing food in the event of a famine.

Light Detection and Ranging, or LIDAR, has become increasingly popular for use in remote sensing. The ability to analyze vegetation and topography elements in distinct three dimensions is made possible by airborne altimetric LiDAR [6,7,8,9,10,11]. Across a wide area of the landscape, this active sensor pulses a laser, measuring the intensity and round-trip times of the returned pulses. These data are then translated into range measurements. Accuracy is obvious and recognized by numerous governments and business sectors with the use of LIDAR technology. Therefore, it is essential to extract data precisely and accurately as a baseline for estimating the output of high-value crops in Butuan City. This will give decision-makers on agricultural vegetation more trustworthy information. Additionally, this will open new avenues for crop-related research and development in the future.

## 2. METHODOLOGY

This section presents the description and profile of the study area and the major processes employed as shown Fig. 2. To generate yield estimation of major crops in Butuan City, Agusan del Norte, Philippines. It has five major processes employed: landcover classification, features extraction, field measurements, development of the allometric model, and yield estimation.

### 2.1 The Study Area

The Butuan City Planning Office's data indicates that the city's total land area is 816.62 km². 48.64% of its total area is made up of agricultural land, 32.82% of forestland, 7.48% of pastureland, and 11.06% of built-up land [12]. It only illustrates that agriculture occupies a large portion of the city's entire territory. Fig. 1 shows the location of the study and its boundaries.

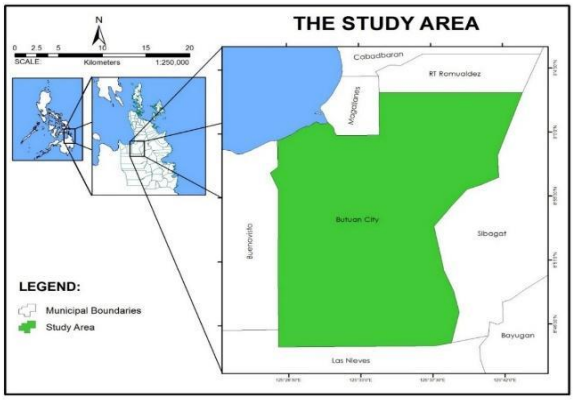


Fig. 1. Map of Butuan city and its boundary.

**2.2 Agricultural Resource Classification**

Pre-processed LiDAR data and color aerial imagery (orthophoto) of Butuan City were the remotely sensed datasets used in this study for the classification of high-value crops. For object-based image analysis, the item was first segmented before being classified. To create meaningful "objects," neighboring pixels were grouped according to their homogeneity through a method known as segmentation [13,14,15,16,17]. The next step involved classifying these items. Several eCognition techniques made it simple to perform both segmentation and classification. Using user-defined rule sets, object-based classification was carried out.

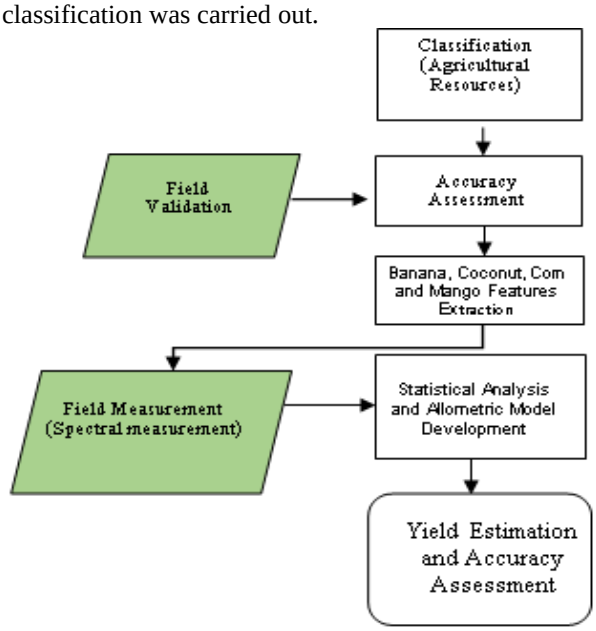


Fig. 2. Process flow of the study.

**2.3 Validation and Accuracy Assessment**

Field validation surveys were carried out to confirm the real land cover existed in the area and to evaluate the accuracy of the classified land cover using the general rule sets produced. The following previous operations were included in the validation process: (a) choosing training/validation points; (b) digitizing road routes; (c) creating field guide maps; and (d) conducting actual field validation surveys. The project's field validation surveys yielded validated points, which were then used to assess the accuracy of the resulting classification using ENVI's classification confusion matrix.

**2.4 Banana, Coconut, Corn, and Mango Feature Extraction**

Mango, banana, coconut, and corn features were taken from the identified land cover and converted to a shapefile for use in a GIS using the eCognition environment. The resources were categorized using the created ruleset, which was then used in the software's process tree. The process of extraction involved choosing the classes to be exported, configuring the export type as shapefile, and exporting the output through the toolbar. Furthermore, a stratified sampling technique was employed to determine the sample site based on the region distribution of each crop, utilizing the attributes that had been extracted.

**2.5 Field Measurement (In situ Spectral Response Measurement of Banana, Coconut, Corn and Mango**

On a clear, sunny day, spectral signature measurements were made at intervals of 9 AM to 2 PM using a USB 4000 Spectrometer[18,19]. Every sample was measured in two minutes after three trials totaling thirty scans each. Every trial contains two light references—before and after—and one black reference. Except for the dark reference, all 30 scans were taken throughout the 2 minutes for these references.

The Ocean OpticsTM Spectrometer was used to measure the reflectance spectra at each sampling point, slightly above the canopy. The sensor has a spectral range of 350 nm to 1000 nm for data detection and recording. The sensor was part of the setup that measured the spectra of the crops. It was placed somewhat above the canopy, put in a makeshift pole, and connected to fiber optics. A laptop computer was linked to the spectrometer, which was used to carry out the scanning process, show the plot of the observed reflectance, and store the reflectance data. There were only three modes of spectral measurements for maize, but five modes of spectral measurement were carried out for each sample crop stage: four on the side of the canopy (i.e., at 45 degrees separation) and one on top of the canopy. It required 20 scans for each mode; the sample's spectral reflectance at that sampling location is represented by the average of those scans. The amount of radiation reflected by the sample crop and the reflected radiation from a "white reference panel" (Ocean Optics LS1 diffused reflectance standard) were the two types of measurements made at each site. Both before and after the sample crops were measured, the white reference panel was measured. All gathered data were converted to Microsoft Excel format and the reflectance was calculated using the equation below.

$$R = \frac{L_{canopy}}{L_{panel}} \; x \; 100\%$$

Eqn. 1. Reflectance equation

where Lpanel is the measured radiance for the calibration panel, Lcanopy is the average measured radiance above the canopy, and R is the canopy reflectance.

**2.6 Statistical Analysis and Allometric Model Development**

Global vegetation indices, such as the Vegetation Condition Index (VCI), which measures plant greenness, the Thermal Condition Index (TCI), which measures temperature, and the Vegetation Health Index (VHI), which is a linear combination of VCI and THI, were used to estimate yield [20,21]. Using ArcMap 10.4 software, an allometric model was created between the actual yield data of the five sample locations per crop and the Vegetation Health Index of the processed image.

Regression analysis was then used to analyze the model and create a yield map for Butuan City.

### 2.7 Yield Estimation and Accuracy Assessment

Using vegetation health index extracted from Landsat 8 OLI/TIRS data using GVI indices, including yield data of the previous planting cycle, a yield estimation was made via regression using Microsoft Excel 365. Crop health analysis was determined using spectral analysis of its chlorophyll content, obtained through a field survey using a USB 4000 spectrometer. This was then compared to a control with standard chlorophyll quantities of crops in areas with known minimal thermal stress

Global vegetation indicators, such as the Vegetation Condition Index (VCI), which measures plant greenness, the Thermal Condition Index (TCI), which measures temperature, and the Vegetation Health Index (VHI), which is a linear combination of VCI and THI, were used to estimate yield [22,23]. The accuracy assessment of the model was performed to assess its suitability for yield estimation. The ratio of the estimated to actual yield of the five sampling regions for each crop—banana, coconut, corn, and mango—was obtained from fieldwork interviews.

## 3. RESULTS AND DISCUSSIONS

### 3.1 Agricultural Resource Classification

Based on the developed methodological procedure, the orthophoto and LiDAR derivatives of Butuan City were subjected to pre-processing before the classification of the crops in the city, and the result is shown in Fig. 3. The findings showed that Butuan City's agricultural resources included bananas, rice, corn, coconuts, mangoes, and oil palm. However, additional non-agricultural land cover characteristics, like water, roads, fallow areas, grasslands, shrublands, sand/bare rock/clay, buildings, and non-agricultural trees, were also included in the classification.

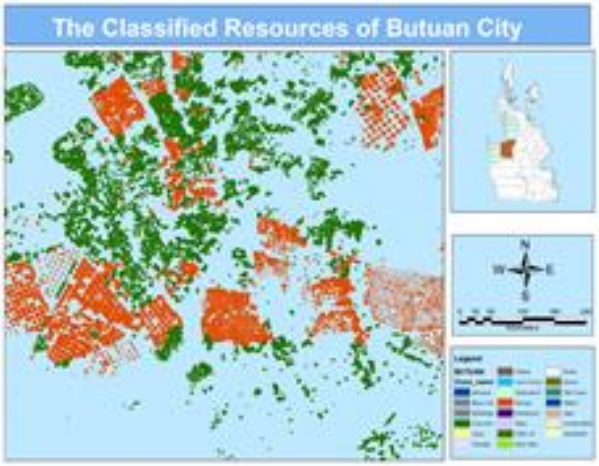


Fig. 3. Classified resources in Butuan city.

As Fig. 4 illustrates. Butuan City's primary agricultural resources included bananas, coconuts, corn, and mangoes. It made up 0.5%, 13.67%, 0.02%, and 2.00% of the area distribution's total classified features, respectively.

Additionally, the degree of accuracy in the resource classification was evaluated. The outcome demonstrates that the created optimized algorithm uses Object-Based Image Analysis (OBIA) classification to extract detailed agricultural resources and provides the best feasible result.

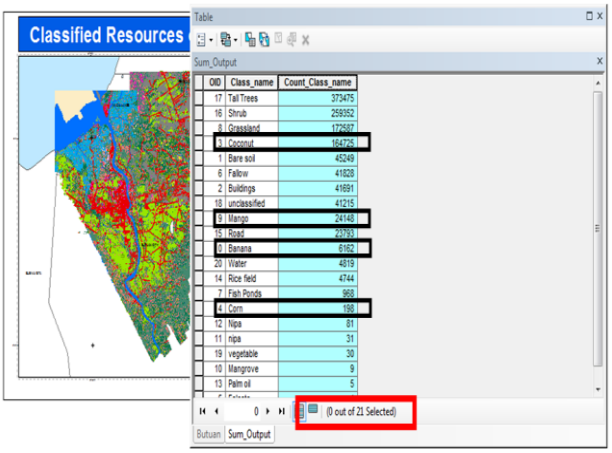


Fig. 4. Summary of areal distribution of classified resources.

As illustrated in Fig. 5, the overall accuracy of the classified detailed resource map created using LiDAR data increased to a high of 94.36%, with the Kappa Index Agreement (KIA) being closest to 93%.

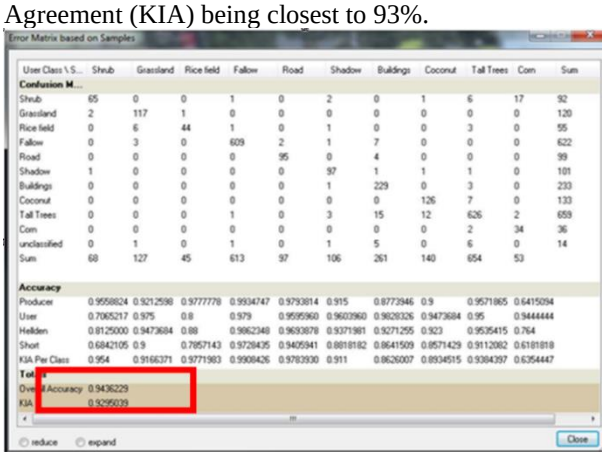


Fig. 5. Accuracy assessment of the classified resources

The general accuracy of earlier research [23,25] results was increased from roughly 72% to 91% for the 1985 map, 76% to 90% for the 1995 map, and 79% to 87% for the 2005 map. This means that the study's accuracy yields very respectable results for thorough classification mapping utilizing LiDAR data and orthophoto.

### 3.2 Banana, Coconut, Corn and Mango Features Extraction

Using eCognition software, features of bananas, coconuts, corn, and mangos were extracted from the classified resources and converted to shapefiles for GIS application and the result is shown in Fig. 5. The retrieved features resulted in 195,233 overall segmented objects, of these, 6,162 (3.15%) were segmented for bananas, 164,725 (84.37%) for coconuts, 198 (1.01%) for corn, and 24,148 (12.36%) for mangos. Among the top 4 major crops in the city, coconut had the highest areal distribution with a total of 4, 357 .15 hectares followed by mango with 203. 32 hectares.

Additionally, using GIS, the minimum, maximum, total, and mean height and crown area values of the banana, coconut, corn, and mango were ascertained. It reveals that the average height of corn, mango, coconuts, and bananas, and 7.64 m, 1.13 m, and 3.92 m, respectively, were found in Butuan City. Banana stems can grow up to 4 or 5 meters tall. According to [26], banana stems can reach up to 4 to 5 meters high. Hence, based on the result

of this study, bananas were considered at the reproductive stage with a 4 m average height.

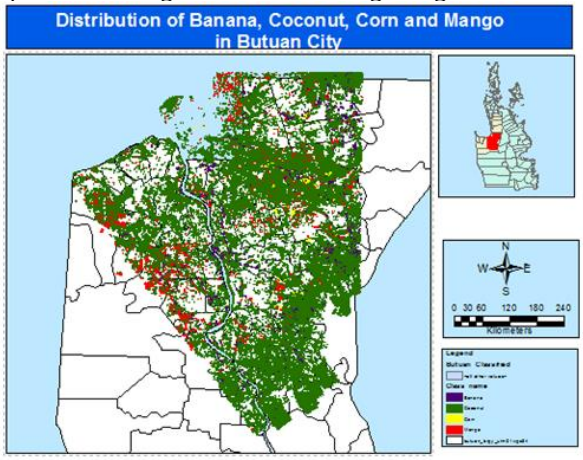


Fig. 6. Extracted banana, coconut, corn, and mango features in Butuan city.

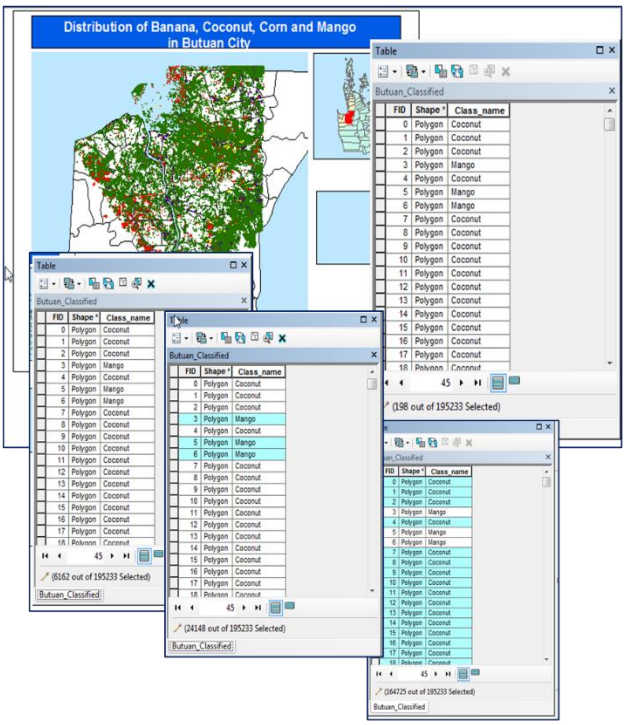


Fig. 7. The attribute tables of extracted features and its distribution

In addition, according to [27], the average height of 7.64 m of coconut was estimated as 16 years old using their developed allometric equation and the result of the corn height shows that the majority of the crops were at the vegetative stage at tassel development. Nutrients and water were in high demand to meet the growth needs. Moreover, the average height of grafted mango is 15 feet [28,29] which conformed to the result of this study.

### 3.3 Development of Allometric Model for Yield and VHI

Using a spectrometer, the spectral reflectance of the banana, coconut, corn, and mango was evaluated during in-situ field measurement to establish their physical attributes. The three EMS sections of the visible region (400–700 nm), near-infrared region (700–1350 nm), and mid-infrared region (1350–2500 nm) are where its spectral reflectance can be found. While NIR has very low absorption, transmittance, and reflectance, and MIR has medium to low transmittance and reflectance, the visible region has low reflectance, high absorption, and minimal transmittance [30].

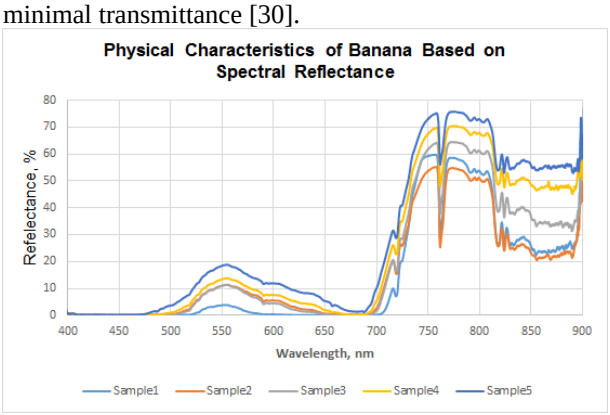


(a) Spectral reflectance of banana

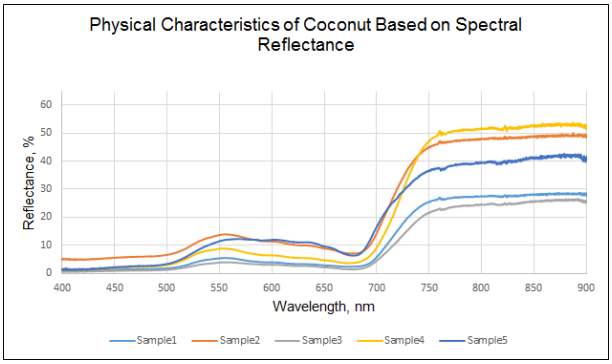


(b) Spectral reflectance of coconut

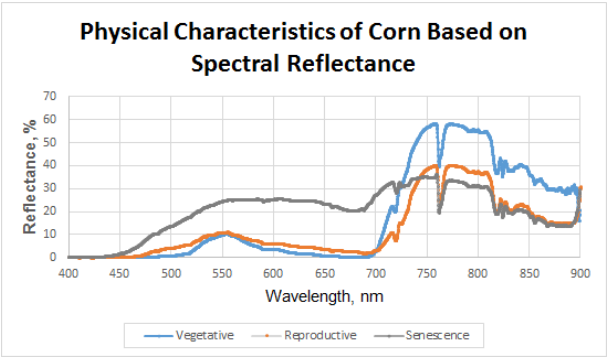


(c) Spectral reflectance of the different stages of corn

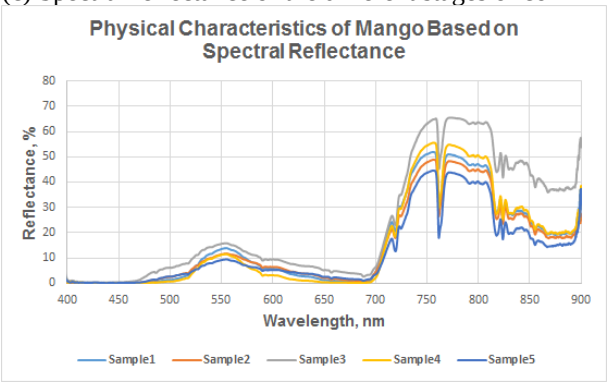


(d) Spectral reflectance of mango

Fig. 8a-8d. Spectral reflectance of the major crops

A healthy green plant's reflectance rises sharply in the near-infrared (NIR), where a plant leaf normally reflects 40–50% of incident energy between 700 and 1300 nm. In the mid-IR, reflectance is controlled by water content. After 1300 nm, healthy vegetation usually absorbs or reflects light energy, with reflectance peaks occurring between 1600 and 2200 nm. Water absorbs between 1400 to 1900 nm, although the precise locations of these bands vary, causing absorptions. As a result, all samples were

regarded as healthy vegetation that complied with the study of [31]. Fig. 8 shows the different spectral responses of each crop.

To generate a yield map in Butuan City, an allometric model was developed between the actual yield data of the five sample points per crop and it Vegetation Health Index of the processed image using ArcMap 10.4 software and the results are shown in Fig. 9.

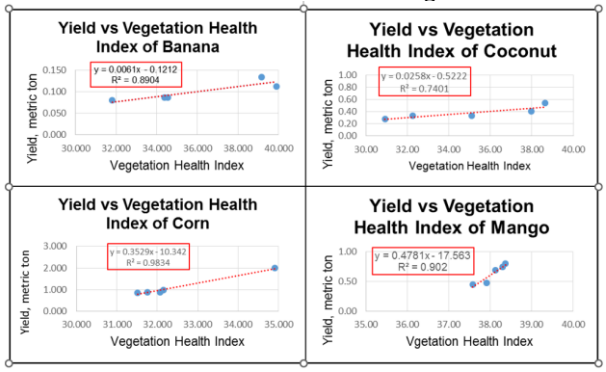


Fig. 9. Allometric model between yield and VHI

Based on the results, vegetation health index and yield had a strong fit linear relationship based on the R2 value of the analysis with 0.8904, 0.7401, 0.9834, and 0.902 for banana, coconut, corn, and mango, respectively. The highlighted red box of the figures was the allometric equation developed to estimate the yield given the vegetation health index and its corresponding R2 value. The model shows that the vegetation health index had a significant impact on yield since the intercept coefficient was negative which means that there is a significant decrease in yield as VHI decreases for both crops.

Moreover, the developed model indicated a strong validity of the regression output since there is a very small significance F value for both crops with a greater probability that the model is valid based on the P-value.

### 3.4 Yield Estimation and Accuracy Assessment

Using the developed allometric equation for yield estimation, maps were produced to illustrate the distribution of the estimated yield of banana, coconut, corn, and mango in Butuan City based on the Vegetation Health Index. Fig. 10 shows the estimated yield distribution of bananas in the city and based on the result; it had an average production of 58.414 tons per hectare.

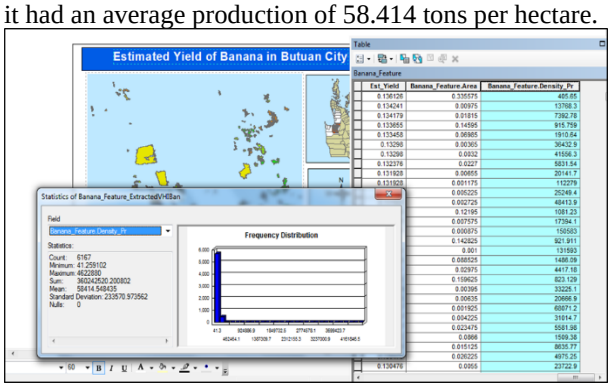


Fig. 10. Estimated yield distribution of banana (ton/ha)

Yields of 15, 20, and up to 45 tons/ha can normally be obtained for the 'Brazilian', 'Bluefields', and 'Cavendish' varieties, respectively [32]. Yields of 84 tons/ha have been reported under optimal conditions. Hence, proper care and maintenance are recommended in banana plantations in Butuan City to attain better yield under good conditions.

Also, the estimated yield of coconut was computed, and the result is shown in Fig. 11. Based on the result, Butuan City had a total estimated coconut production of about 164.913 metric tons with an average yield of 1,001.15 tons/ha with a comparative result to the PCA-Caraga Report (Copra Production 2017-2022) of 1,045.6 tons/ha. On the other hand, the estimated yield distribution of corn in Butuan City is shown in Fig. 12. Most of the corn farmers in Butuan City were planting Hybrid corn varieties. The result shows that there was an estimated total yield of 1.6 metric tons with an average yield of 8.48 tons/ha which had a comparative result to the average hybrid corn yield in Mindoro Occidental at 5.5-9.0 tons/ha [33,34].

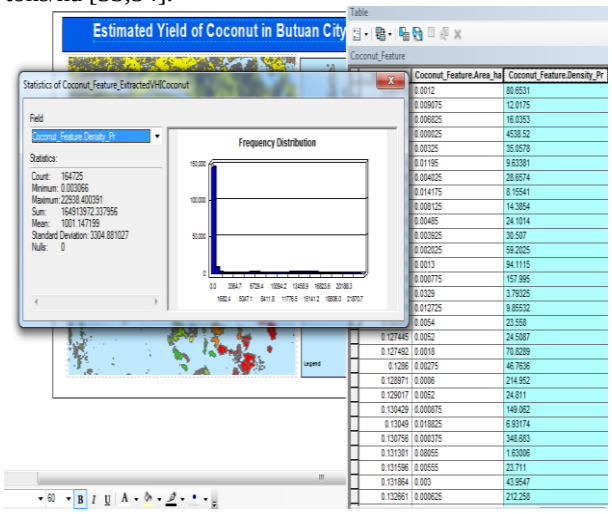


Fig. 11. Estimated yield distribution of coconut ton/ha)

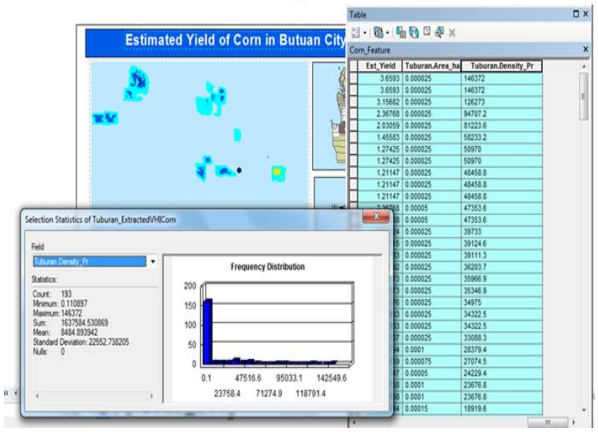


Fig. 12. Estimated yield distribution of corn (ton/ha)

Moreover, the estimated yield of the extracted mango in Butuan City was computed and the result was mapped as shown in Fig. 13. Based on the result, there was an estimated total production of 180.882 metric tons with an average yield of 1.256 tons/ha. The 2017-2022 report of the City Agriculture Office stated that the average yield of mango in the city was about 1.5 tons/ha. Thus, its yield data estimation has an accuracy of 83.4%.

To determine the fitness of the model for yield estimation, an accuracy assessment was performed. Assessment was done by getting the ratio of the estimated yield to the actual yield of banana, coconut, corn, and mango collected during fieldwork interviews of the five sampling areas per crop.

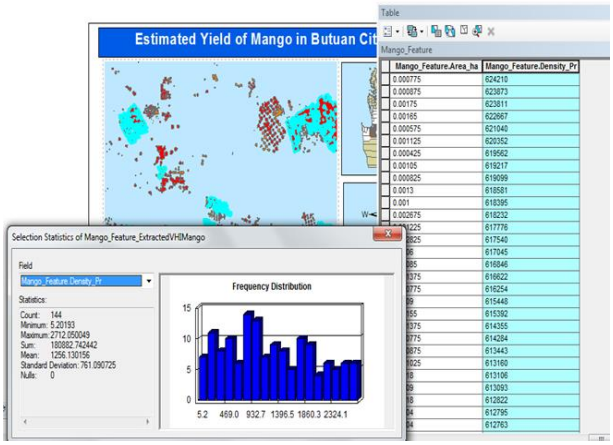

Fig. 13. Estimated yield distribution of mango (ton/ha)

Based on the result, the model had an accuracy of 84.5%, 87.9%, 72.5%, and 83.7% for banana, coconut, corn, and mango, respectively. The resulting accuracy shows acceptable results for yield estimation using LiDAR data coupled with Landsat 8 images.

## 4. CONCLUSION

The study's findings led the researchers to the conclusion that remote sensing may be used to estimate the yield of bananas, coconuts, corn, and mangoes. The various resources in the city were categorized using object-based classification of high-value crops using an improved SVM model with LiDAR data and Orthophoto. An important yield estimate was produced by the devised, optimized method that was used in the classification and produced an extremely high overall accuracy. Yield estimation was produced with sufficient practical use of LiDAR data (Normalized Digital Surface Mod [nDSM]) and other remote sensing data; the resulting accuracy indicates satisfactory results for yield estimation using LiDAR data coupled with Landsat 8 images.

Thus, the project's output was valuable for several purposes, including planning, observing, and evaluating the physiological structure for resource management, economics, food security, technology application, and other purposes.

## 5. REFERENCES


[1] Mindanao Strategic Development Framework,website: *https://www.neda.gov.ph/wp-content/uploads/2013/10/MSDF_finalforweb_2010-2020.pdf* (accessed on 20 June 2024).

[2] FAO, "Climate Smart Agriculture Sourcebook," Food and Agriculture Organization of the United Nations website: *https://www.fao.org/climate-smart-agriculture-sourcebook/en/* (accessed on 01 June 2024).

[3] I. F. P. Research Institute (IFPRI), "Climate change: Impact on agriculture and costs of adaptation," 2009. doi: 10.2499/0896295354.

[4] J. P. Aryal, T. B. Sapkota, R. Khurana, A. Khatri-Chhetri, D. B. Rahut, and M. L. Jat, "Climate change and agriculture in South Asia: adaptation options in smallholder production systems," *Environ. Dev. Sustain.*, vol. 22, no. 6, pp. 5045–5075, Aug. 2020, doi: 10.1007/s10668-019-00414-4.

[5] "CLIPPINGS-FOR-APRIL-27-2024"website: https://www.da.gov.ph/wp-content/uploads/2024/04/CLIPPINGS-FOR-APRIL-27-2024.pdf (accessed on 25 May 2024).

[6] C. A. Mciver and M. Stefanou, "Naval Postgraduate School Monterey, California Thesis Approved for public release. Distribution is unlimited. Spectral LiDAR Analysis and Terrain Classification in a Semi-Urban Environment," 2017.

[7] M. A. Wulder *et al.*, "Lidar sampling for large-area forest characterization: A review," *Remote Sensing of Environment*, vol. 121. pp. 196–209, Jun. 2012. doi: 10.1016/j.rse.2012.02.001.

[8]R. W. Kulawardhana, S. C. Popescu, and R. A. Feagin, "Airborne lidar remote sensing applications in non-forested short stature environments: A review," *Annals of Forest Research*, vol. 60, no. 1. Editura Silvica, pp. 127–150, 2017. doi: 10.15287/afr.2016.719.

[9] M. A. Salopek and N. Huntingdon, "The Use of LiDAR Remote Sensing in Measuring Forest Carbon Stocks," 2013.

[10] M. J. Micheletto, C. I. Chesñevar, and R. Santos, "Methods and Applications of 3D Ground Crop Analysis Using LiDAR Technology: A Survey," *Sensors*, vol. 23, no. 16. Multidisciplinary Digital Publishing Institute (MDPI), Aug. 01, 2023. doi: 10.3390/s23167212.

[11] K. Schmid *et al.*, "Lidar 101: An Introduction to Lidar Technology, Data, and Applications," 2012. [Online]. Available: www.csc.noaa.gov

[12] NEDA, "Master Plan for the Sustainable Urban Infrastructure Development in Butuan City 2020, website: https://nro13.neda.gov.ph/wp-content/uploads/2021/10/Master-Plan.pdf" (accessed on 14 May 2024).

[13] R. T. Alberto *et al.*, "Object Based Agricultural Land Cover Classification Map of Shadowed Areas From Aerial Image and Lidar Data Using Support Vector Machine," *ISPRS Ann. Photogramm. Remote Sens. Spat. Inf. Sci.*, vol. III–7, no. July, pp. 45–50, 2016, doi: 10.5194/isprsannals-iii-7-45-2016.

[14] L. C. G. David, S. M. Sarte, J. R. V. Laguerta, and A. H. Ballado, "Feature selection in LiDAR height metrics using decision tree for SVM classification: Application in agricultural resources mapping," *37th Asian Conf. Remote Sensing, ACRS 2016*, vol. 1, pp. 178–185, 2016.

[15] J. Zhang, X. Lin, and X. Ning, "SVM-Based *classification* of segmented airborne LiDAR point clouds in urban areas," *Remote Sens.*, vol. 5, no. 8, pp. 3749–3775, 2013, doi: 10.3390/rs5083749.

[16] J. G. Luzorata, A. E. Bocobo, L. M. Detera, N. J. B. Pocong, and A. P. Sajonia, "Assessment of Land Use Land Cover Classification using Support Vector Machine and Random Forest Techniques in the Agusan River Basin through Geospatial Techniques," *International Exchange and Innovation Conference on Engineering and Sciences, Kyushu University*, vol. 9, pp. 240–246, 2023, doi: 10.5109/7157978.

[17] E. Ekren, "Investigation of Land Cover Change in Kahramanmaras Province (Turkey)," *International Exchange and Innovation Conference on Engineering and Sciences, Kyushu University,2022* pp. 407–411, doi: 10.5109/5909125.

[18] D. M. G. Dela Torre *et al.*, "Development of field sampling protocols for a spectral library of agricultural crops in the Philippines," *37th Asian Conf. Remote Sensing, ACRS 2016*, vol. 3, pp. 2074–2079, 2016.

[19] O. Optics, “HR2000 + High-speed Fiber Optic Spectrometer Installation and Operation Manual,” *World*, no. 294.
[20] V. A. Bento, I. F. Trigo, C. M. Gouveia, and C. C. DaCamara, “Contribution of Land Surface Temperature (TCI) to Vegetation Health Index: A comparative study using clear sky and all-weather climate data records,” *Remote Sens.*, vol. 10, no. 9, 2018, doi: 10.3390/rs10091324.
[21] H. T. Pham, J. Awange, M. Kuhn, B. Van Nguyen, and L. K. Bui, “Enhancing Crop Yield Prediction Utilizing Machine Learning on Satellite-Based Vegetation Health Indices,” *Sensors*, vol. 22, no. 3, pp. 1–19, 2022, doi: 10.3390/s22030719.
[22] J. R. F. Mirandilla, M. Yamashita, M. Yoshimura, and E. C. Paringit, “Leaf Spectral Analysis for Detection and Differentiation of Three Major Rice Diseases in the Philippines,” *Remote Sens.*, vol. 15, no. 12, 2023, doi: 10.3390/rs15123058.
[23] R. A, “Using AVHRR-Based Vegetation Health Indices For Estimation Of Potato Yield In Bangladesh,” *J. Civ. Environ. Eng.*, vol. 02, no. 03, pp. 10–13, 2012, doi: 10.4172/2165-784x.1000111.
[24] R. Manandhar, I. O. A. Odehi, and T. Ancevt, “Improving the accuracy of land use and land cover classification of landsat data using post-classification enhancement,” *Remote Sens.*, vol. 1, no. 3, pp. 330–344, 2009, doi: 10.3390/rs1030330.
[25] P. Dash, S. L. Sanders, P. Parajuli, and Y. Ouyang, “Improving the Accuracy of Land Use and Land Cover Classification of Landsat Data in an Agricultural Watershed,” *Remote Sens.*, vol. 15, no. 16, pp. 1–24, 2023, doi: 10.3390/rs15164020.
[26] Das, B., Patnaik, S. K., Bordoloi, R., Paul, A., & Tripathi, O. P. (2022). Prediction of forest aboveground biomass using an integrated approach of space-based parameters, and forest inventory data. Geology, Ecology, and Landscapes, 1–13. https://doi.org/10.1080/24749508.2022.2139484
[27] “Sawadogo, L., Savadogo, P., Tiveau, D. et al. Allometric prediction of above-ground biomass of eleven woody tree species in the Sudanian savanna-woodland of West Africa. Journal of Forestry Research 21, 475–481 (2010). https://doi.org/10.1007/s11676-010-0101-4.
[28] A. K. Karna, “Studies of Grafting Height on Success of Softwood Grafting in Mango (Mangifera indica L.),” *Int. J. Pure Appl. Biosci.*, vol. 6, no. 6, pp. 435–438, 2018, doi: 10.18782/2320-7051.7058.
[29] W. Luo *et al.*, “Comparative RNA-seq analysis reveals candidate genes associated with fruit set in pumpkin,” *Sci. Hortic. (Amsterdam).*, vol. 288, no. April, 2021, doi: 10.1016/j.scienta.2021.110255.
[30] P. Piro, M. Porti, S. Veltri, E. Lupo, and M. Moroni, “Hyperspectral monitoring of green roof vegetation health state in sub-mediterranean climate: Preliminary results,” *Sensors (Switzerland)*, vol. 17, no. 4, 2017, doi: 10.3390/s17040662.
[31] K. Pfitzner, A. Bollhöfer, and G. Carr, “A standard design for collecting vegetation reference spectra: Implementation and implications for data sharing,” *J. Spat. Sci.*, vol. 51, no. 2, pp. 79–92, 2006, doi: 10.1080/14498596.2006.9635083.
[32] K. Nyombi, *Understanding growth of East* Africa *highland banana: experiments and simulation.*, no. January 2010. website: https://edepot.wur.nl/132641 (accessed on 10 June 2024).
[33] D. K. S. Swastika *et al.*, *Maize in Indonesia: production systems, constraints and research priorities*, no. January. 2004. [Online]. Available: http://books.google.com/books?hl=en&lr=&id=bZ-t7dHwvHAC&pgis=1 (accessed on 24 May 2024)
[34] L. K. P. G. A *et al.*, “Growth and Yield of Four Maize Varieties as Affected By Climatic Conditions During Off-Season Planting Months in Los Baños , Philippines,” vol. 46, no. December, pp. 27–37, 2021.